Dynamic tomography and ROI reconstruction

L. Desbat, C. Mennessier, R. Clackdoyle

TIMC-IMAG, UMR 5525, UJF-Grenoble 1, France
LHC UMR 5516, St Etienne, France

DROITE meeting - Valpré, Lyon- October 25th 2012

Dynamic tomography: motivation

- Cardiac CT, [Li *et al.* , 1995, Grangeat *et al.* , 2002], gating methods [Kachelriess & Kalender, 1998, Kachelriess *et al.* , 2000, Flohr & Ohnesorge, 2001, Gilland *et al.* , 2002]
- Nuclear imaging acquisition (PET or SPECT) with stochastic modeling including movement
- C-arm for interventional imaging [Krimski & et al, 2005]
- Outstanding presentations at CT2012: sessions M1, M3, T1, W1, ...

Summary

- Analytic reconstruction

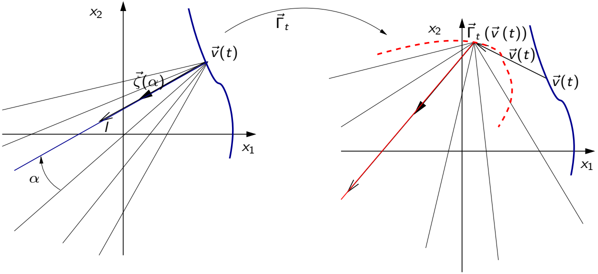

- Region Of Interest reconstruction

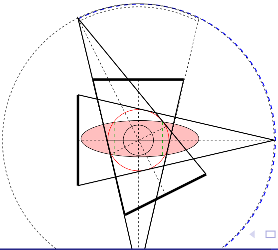

Outline

Divergent geometry, 2D Fan Beam

- $\mu : \mathbb{R}^d \to \mathbb{R}$ is the (regular) function to be reconstructed ($d = 2, 3$)
- $\vec{v} \in \mathbb{R}^d$ denotes a point (an X-ray source position in X-ray CT), and $\vec{\zeta} \in \mathbb{S}^{d-1}$ a unit vector (in the direction from the source to the detector in X-ray CT),
- the Divergent Beam transform is defined by

$$\mathcal{D}\mu\left(\vec{v}, \vec{\zeta}\right) \stackrel{\text{def}}{=} \int_0^{+\infty} \mu\left(\vec{v} + l\vec{\zeta}\right) dl$$

- $\mathcal{C} = \{\vec{v}(t), t \in T \subset \mathbb{R}\}$ in $\mathbb{R}^d$ is the source trajectory.
- 2D fan beam data $d(t, \alpha) = \mathcal{D}\mu\left(\vec{v}(t), \vec{\zeta}(\alpha)\right)$ with $\vec{\zeta}(\alpha) = (\cos\alpha, \sin\alpha)$, $\alpha \in [0, 2\pi[$

Movement model

- $\mu(t,\vec{x})$ depends on t
- Assumption $\mu(t,\vec{x})$ behaves like $\mu\left(\vec{\Gamma}_t(\vec{x})\right)$ where $\vec{\Gamma}_t$ is a time dependent diffeomorphic deformation, i.e. a smooth bijective mapping on the space $\mathbb{R}^d$, $d \in \{2,3\}$:

$$\begin{array}{cccc} \vec{\Gamma}_t : & \mathbb{R}^d & \longrightarrow & \mathbb{R}^d \\ & \vec{x} & \longrightarrow & \vec{\Gamma}_t(\vec{x}) \end{array}.$$

  introduced by Crawford et al [Crawford *et al.* , 1996]
- Mass conservation $\forall \Omega \subset \mathbb{R}^d$

$$\int_\Omega \mu\left(\vec{\Gamma}_t(\vec{x})\right) |\det J_{\vec{\Gamma}_t}(\vec{x})| d\vec{x} = \int_{\vec{\Gamma}_t(\Omega)} \mu(\vec{y})\, d\vec{y}$$

  where $\det J_{\vec{\Gamma}_t}(\vec{x})$ is the determinant of $J_{\vec{\Gamma}_t}(\vec{x})$ the Jacobian matrix of $\vec{\Gamma}_t$ at $\vec{x}$. We suppose from now that $\mu(t,\vec{x})$ is in fact $\mu_{\vec{\Gamma}_t}(\vec{x}) = \mu\left(\vec{\Gamma}_t(\vec{x})\right) |\det J_{\vec{\Gamma}_t}(\vec{x})|$

Dynamic Tomography model

- We suppose from now that $\mu(t,\vec{x})$ is in fact $\mu_{\vec{\Gamma}_t}(\vec{x}) = \mu\left(\vec{\Gamma}_t(\vec{x})\right) |\det J_{\vec{\Gamma}_t}(\vec{x})|$
- We would like to identify μ from

$$\mathcal{D}\mu_{\vec{\Gamma}_t}(\vec{v}(t),\vec{\zeta}) = \int_{\mathbb{R}} \mu\left(\vec{\Gamma}_t\left(\vec{v}(t) + l\vec{\zeta}\right)\right) |\det J_{\vec{\Gamma}_t}(\vec{v}(t) + l\vec{\zeta})| dl$$

for some source trajectory $\vec{v}(t), t \in T$, line directions $\vec{\zeta} \in \mathbb{S}^{d-1}$ and $\vec{\Gamma}_t$ *known*.

Acquisition geometry preservation

The beams $\vec{v}(t) + \mathbb{R}^+\vec{\zeta}$ (integration half line) at t are transformed by $\vec{\Gamma}_t$ into a half lines.

- the source $\vec{v}(t)$ is transformed into a new source point $\vec{\Gamma}_t\left(\vec{v}(t)\right)$
- the line direction $\vec{\zeta}$ is transformed into a new direction denoted $\vec{\Sigma}_t(\vec{\zeta})$ where $\vec{\Sigma}_t$ is a diffeomorphism on the unit sphere (smooth bijection on the sphere):

$$\begin{array}{rccc} \vec{\Sigma}_t : & \mathbb{S}^{d-1} & \longrightarrow & \mathbb{S}^{d-1} \\ & \vec{\zeta} & \longrightarrow & \vec{\Sigma}_t(\vec{\zeta}) \end{array}.$$

Thus a deformation preserving the divergent geometry satisfies

$$\vec{\Gamma}_t\left(\vec{v}(t) + \mathbb{R}^+\vec{\zeta}\right) = \vec{\Gamma}_t\left(\vec{v}(t)\right) + \mathbb{R}^+\vec{\Sigma}_t(\vec{\zeta}).$$

Geometry conservation

Modeling the deformation along each half line $\vec{v}(t) + \mathbb{R}^+\vec{\zeta}$

$$\begin{array}{rccc} \gamma_{t,\vec{\zeta}}: & \mathbb{R}^+ & \longrightarrow & \mathbb{R}^+ \\ & l & \longrightarrow & \gamma_{t,\vec{\zeta}}(l) \end{array}.$$

We have, $\forall l \in \mathbb{R}^+$, $\forall \vec{\zeta} \in \mathbb{S}^{d-1}$,

$$\vec{\Gamma}_t\left(\vec{v}(t) + l\vec{\zeta}\right) = \vec{\Gamma}_t\left(\vec{v}(t)\right) + \gamma_{t,\vec{\zeta}}(l)\vec{\Sigma}_t(\vec{\zeta}).$$

Clearly for $\vec{\Gamma}_t$ to be smooth and bijective, $\gamma_{t,\vec{\zeta}}$ must be a strictly monotonic smooth function and $\gamma_{t,\vec{\zeta}}(0) = 0$. $\left(\gamma_{t,\vec{\zeta}}, \vec{\Sigma}_t\right)$ is the change of the spherical variables $(l, \vec{\zeta}) \in \mathbb{R}^+ \times \mathbb{S}^{d-1}$ centered on $\vec{v}(t)$ to the spherical variables $(\gamma_{t,\vec{\zeta}}(l), \vec{\Sigma}_t(\vec{\zeta})) \in \mathbb{R}^+ \times \mathbb{S}^{d-1}$ centered on $\vec{\Gamma}_t\left(\vec{v}(t)\right)$, associated to $\vec{\Gamma}_t$.

Mass conservation in $\mathbb{R}^d$

if

$$\mu_{\vec{\Gamma}_t}\left(\vec{v}(t)+l\vec{\zeta}\right)$$
$$=\mu\left(\vec{\Gamma}_t\left(\vec{v}(t)\right)+\gamma_{t,\vec{\zeta}}(l)\vec{\Sigma}_t(\vec{\zeta})\right)|\gamma'_{t,\vec{\zeta}}(l)||J_{\vec{\Sigma}_t}(\vec{\zeta})|\frac{\gamma^{d-1}_{t,\vec{\zeta}}(l)}{l^{d-1}}$$

we have ($\vec{\Gamma}_t$ is a change of variable on $\mathbb{R}^d$).

$$\int_{[l_1,l_2]\times\Omega_S}\mu_{\vec{\Gamma}_t}\left(\vec{v}(t)+l\vec{\zeta}\right)l^{d-1}dld\vec{\zeta}$$
$$=\int_{[l_1,l_2]\times\Omega_S}\mu\left(\vec{\Gamma}_t\left(\vec{v}(t)\right)+\gamma_{t,\vec{\zeta}}(l)\vec{\Sigma}_t(\vec{\zeta})\right)$$
$$|\gamma'_{t,\vec{\zeta}}(l)||J_{\vec{\Sigma}_t}(\vec{\zeta})|\frac{\gamma^{d-1}_{t,\vec{\zeta}}(l)}{l^{d-1}}l^{d-1}dld\vec{\zeta}$$
$$=\int_{\left[\gamma_{t,\vec{\zeta}}(l_1),\gamma_{t,\vec{\zeta}}(l_2)\right]\times\vec{\Sigma}_t(\Omega_S)}\mu\left(\vec{\Gamma}_t\left(\vec{v}(t)\right)+u\vec{\vartheta}\right)u^{d-1}dud\vec{\vartheta}$$

Mass conservation in $\mathbb{R}^d$

the x-ray beam between the source and the detector is some region $\Omega_{\vec{v}(t),\vec{\zeta}}$ (a "tube") of approximately constant photon flux,
$\vec{\Gamma}_t$ transforms the region $\Omega_{\vec{v}(t),\vec{\zeta}}$ around the line $\vec{v}(t)+\mathbb{R}^+\vec{\zeta}$ into $\vec{\Gamma}_t\left(\Omega_{\vec{v}(t),\vec{\zeta}}\right)$ around the line $\vec{\Gamma}_t\left(\vec{v}(t)\right)+\mathbb{R}^+\vec{\Sigma}_t(\vec{\zeta})$.

$$
\begin{aligned}
& \Omega_S \int_{\mathbb{R}^+} \mu_{\vec{\Gamma}_t}\left(\vec{v}(t)+l\vec{\zeta}\right) dl \\
\approx & \int_{\Omega_{\vec{v}(t),\vec{\zeta}}} \mu_{\vec{\Gamma}_t}\left(\vec{v}(t)+l\vec{\zeta}\right) l^{d-1} dl d\vec{\zeta} \\
= & \int_{\vec{\Gamma}_t\left(\Omega_{\vec{v}(t),\vec{\zeta}}\right)} \mu\left(\vec{\Gamma}_t\left(\vec{v}(t)\right)+u\vec{\vartheta}\right) u^{d-1} du d\vec{\vartheta} \\
\approx & \mu_{\vec{\Gamma}_t}(\Omega_S) \int_{\mathbb{R}^+} \mu\left(\vec{\Gamma}_t\left(\vec{v}(t)\right)+l\vec{\Sigma}_t(\vec{\zeta})\right) dl
\end{aligned}
$$

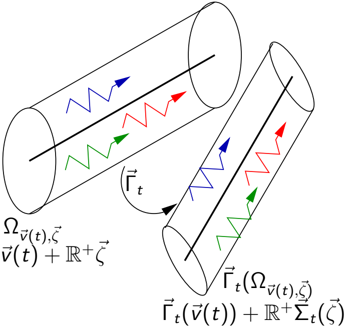

Mass and geometry conservation, rebinning formula

Dynamic rebinning formula

If $\vec{\Gamma}_t$ preserves both the divergent geometry and the mass then

$$\mathcal{D}\mu_{\vec{\Gamma}_t}\left(\vec{v}(t),\vec{\zeta}\right) = c_{t,\vec{\zeta}}\mathcal{D}\mu\left(\vec{\Gamma}_t\left(\vec{v}(t)\right),\vec{\Sigma}_t(\vec{\zeta})\right)$$

2D ROI reconstruction with DBP

$H_\alpha \mu$ the Hilbert transform of μ in the direction α is defined by

$$\begin{array}{rcl} H_{\vec{\zeta}(\alpha)}\mu : \mathbb{R}^2 & \longrightarrow & \mathbb{R} \\ \vec{x} & \longrightarrow & H_{\vec{\zeta}(\alpha)}\mu(\vec{x}) \stackrel{\text{def}}{=} \int_{\mathbb{R}} \mu(\vec{x} - u\vec{\zeta}(\alpha))h(u)du = \int_{\mathbb{R}} \frac{\mu(\vec{x}-u\vec{\zeta}(\alpha))}{\pi u} du \end{array}$$

The backprojection of the derivative of the parallel projections satisfies the equality

$$b_{\alpha,\alpha+\pi}(\vec{x}) \stackrel{\text{def}}{=} \frac{1}{\pi} \int_{\alpha}^{\alpha+\pi} \frac{\partial}{\partial s} p(\phi, \vec{x} \cdot \vec{\theta}) d\phi = 2H_{\vec{\zeta}(\alpha)}\mu(\vec{x})$$

2D ROI reconstruction with DBP (FB)

The derivative according to the trajectory parameter t of the Fan Beam projection is defined

$$g_D\left(\vec{v}(t), \phi\right) \stackrel{\text{def}}{=} \frac{\partial}{\partial t} g\left(\vec{v}(t), \phi\right)$$

Let $\overset{<}{b}_{t_1,t_2}$ be the back projection of g_D on $[t_1, t_2] \subset T$

$$\overset{<}{b}_{t_1,t_2}(\vec{x}) \stackrel{\text{def}}{=} \frac{1}{\pi} \int_{t_1}^{t_2} \frac{1}{||\vec{x} - \vec{v}_t||} g_D\left(\vec{v}(t), \phi\right)|_{\phi = arg(\vec{x} - \vec{v}_t)} dt$$

Then [Clackdoyle & Defrise, 2010]

$$\overset{<}{b}_{t_1,t_2}(\vec{x}) = 2H_{\vec{v}_{t_1} - \vec{v}_{t_2}} \mu(\vec{x}) \text{ for } \vec{x} \in [\vec{v}_{t_1}, \vec{v}_{t_2}]$$

Inversion of the finite Hilbert Transform

Let $[\vec{y}_1, \vec{y}_2]$ be the intersction of the segment $[\vec{v}_{t_1}, \vec{v}_{t_2}]$ with a convex containing the support of μ. If $H_{\vec{v}_{t_1}-\vec{v}_{t_2}}\mu(\vec{y})$ is known for $\vec{y}$ on a segment $[\vec{y}_{1-}, \vec{y}_{2+}]$ a bit larger than $[\vec{y}_1, \vec{y}_2]$, then $\mu(\vec{x})$ can be reconstructed from $H_{\vec{v}_{t_1}-\vec{v}_{t_2}}\mu(\vec{y})$ given for $\forall \vec{y} \in [\vec{y}_{1-}, \vec{y}_{2+}] (\supset [\vec{y}_1, \vec{y}_2] \supset [\vec{v}_{t_1}, \vec{v}_{t_2}])$.

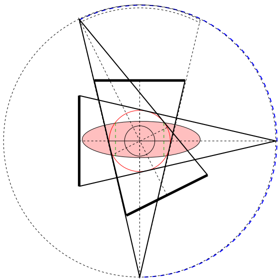

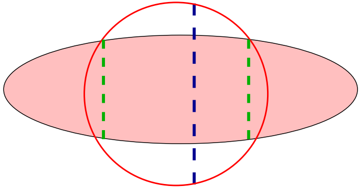

Numerical experiments: dynamic phantom

The phantom μ is an image (linear combination of pixel indicators). $\mu_{\vec{\Gamma}_t}$ is dynamically deformed

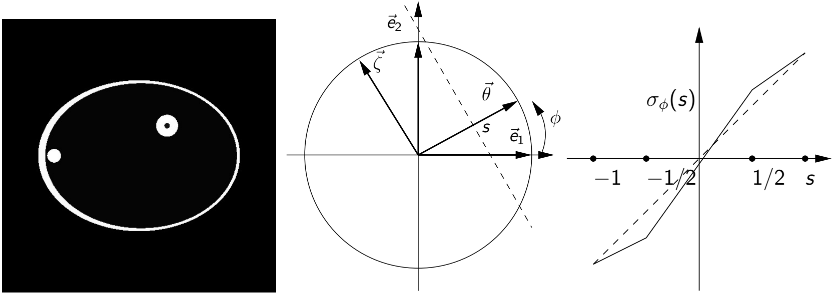

Figure: Left: reference phantom ; right: deformation γ_ϕ on the s axis

420 angular projections, 256 translations $p(\phi, s) = \int \mu_{\vec{\Gamma}_\phi}(s\vec{\theta} + l\vec{\zeta})dl$

$$\vec{\Gamma}_\phi\left(s\vec{\theta}(\phi) + l\vec{\zeta}(\phi)\right) = \sigma_\phi(s)\vec{\theta}(\phi) + l\vec{\zeta}(\phi)$$

Numerical experiments: dynamic phantom

The phantom μ is an image (linear combination of pixel indicators).
$\mu_{\vec{\Gamma}_t}$ is dynamically deformed

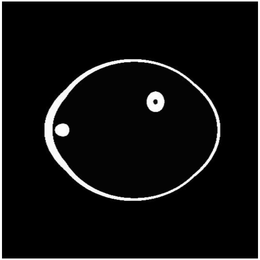

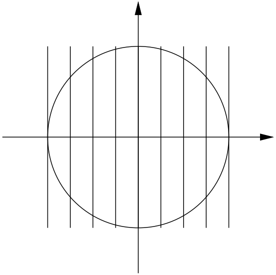

Figure: Dynamic Phantom $\phi = 0$

Numerical experiments: dynamic phantom

The phantom μ is an image (linear combination of pixel indicators).
$\mu_{\vec{\Gamma}_t}$ is dynamically deformed

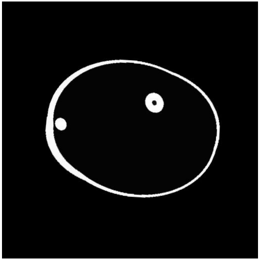

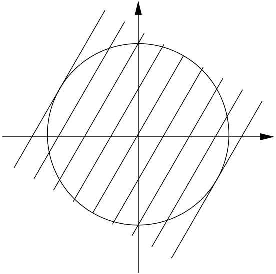

Figure: Dynamic Phantom $\phi = \frac{\pi}{6}$

Numerical experiments: dynamic phantom

The phantom μ is an image (linear combination of pixel indicators).
$\mu_{\vec{\Gamma}_t}$ is dynamically deformed

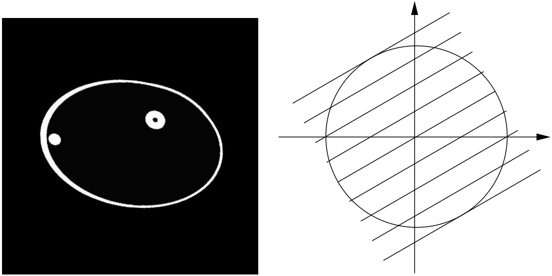

Figure: Dynamic Phantom $\phi = \frac{\pi}{3}$

Numerical experiments: dynamic phantom

The phantom μ is an image (linear combination of pixel indicators).
$\mu_{\vec{\Gamma}_t}$ is dynamically deformed

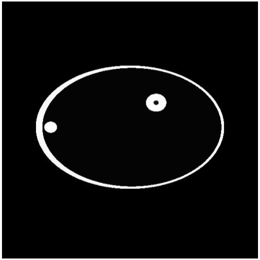

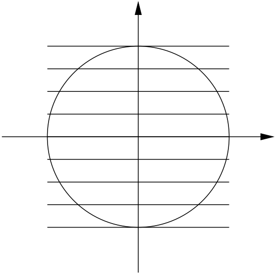

Figure: Dynamic Phanto $\phi = \frac{\pi}{2}$

Numerical experiments : dynamic phantom

The phantom μ is an image (linear combination of pixel indicators).
$\mu_{\vec{\Gamma}_t}$ is dynamically deformed

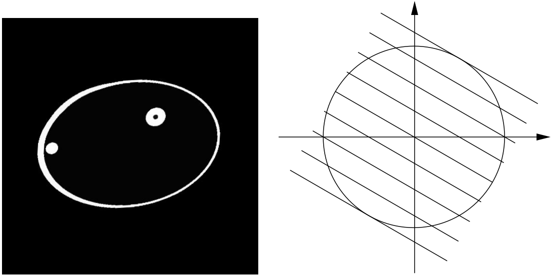

Figure: Dynamic Phantom $\phi = 2\frac{\pi}{3}$

Numerical experiments: dynamic phantom

The phantom μ is an image (linear combination of pixel indicators).
$\mu_{\vec{\Gamma}_t}$ is dynamically deformed

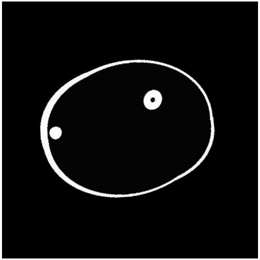

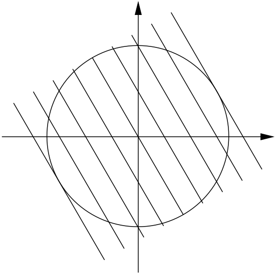

Figure: Dynamic Phantom $\phi = 5\frac{\pi}{6}$

Numerical experiments: dynamic phantom

The phantom μ is an image (linear combination of pixel indicators).
$\mu_{\vec{\Gamma}_t}$ is dynamically deformed

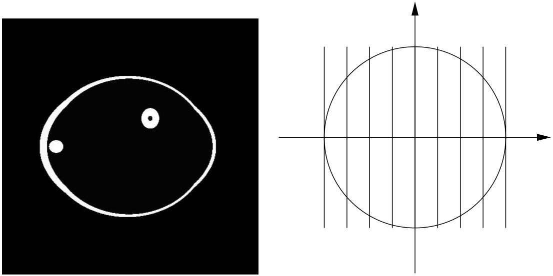

Figure: Dynamic Phantom $\phi = \pi - \Delta\phi$

DBP reconstructions from full scann

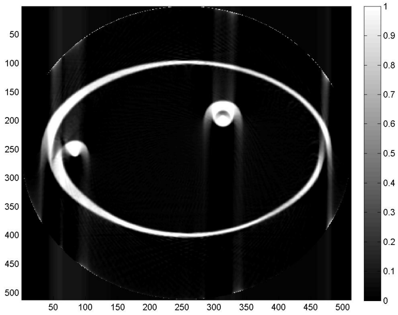

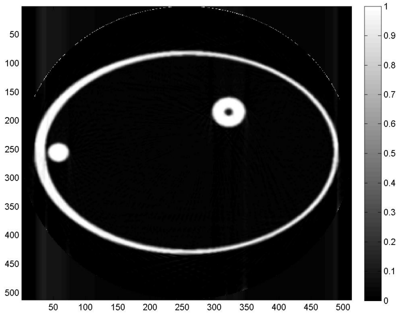

Figure: Left: NO compensation ; Right: Compensation (rebinning)

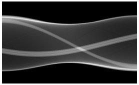

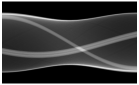

DBP reconstructions from truncated projections

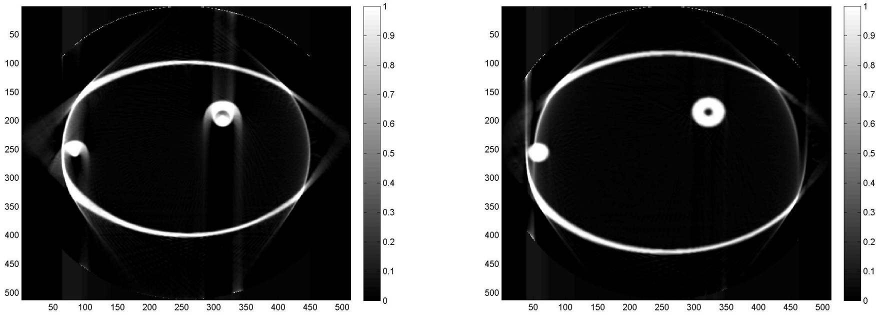

Figure: Left: NO compensation ; Right: Compensation (rebinning)

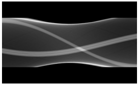

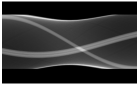

SL: DBP reconstructions from full parallel scann

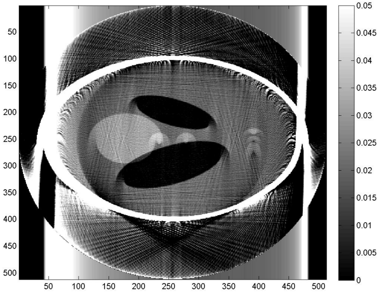

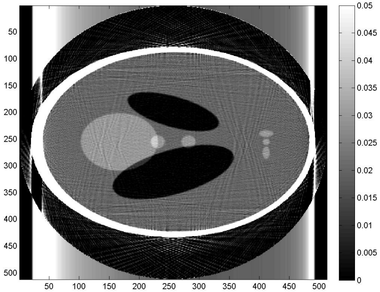

Left: NO compensation ; Right: Compensation (rebinning)

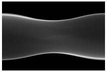

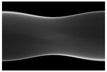

768 angular projections, 512 translations

DBP reconstructions from truncated projections

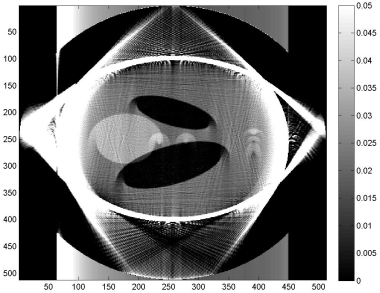

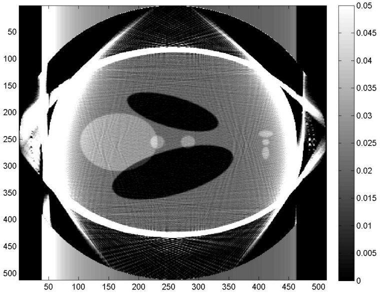

Left: NO compensation ; Right: Compensation (rebinning)

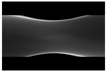

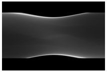

768 angular projections, 512 translations

Numerical experiments: dynamic phantom

The phantom μ is a Shepp and Logan pixel image (linear combination of pixel indicators).

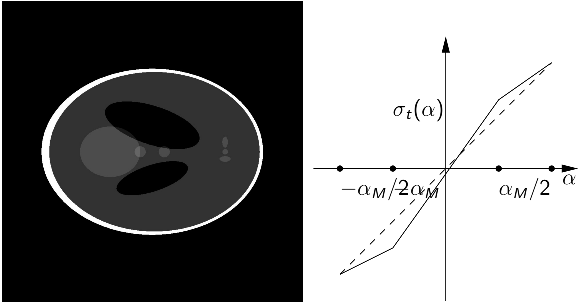

Figure: Reference phantom ; right: deformation γ_t on the α axis

$$\int \mu_{\vec{\Gamma}_t}\left(\vec{v}(t) + l\vec{\zeta}\right) dl$$

$$\vec{\Gamma}_t\left(\vec{v}(t) + l\vec{\zeta}(\alpha)\right) = \vec{v}(t) + l\vec{\zeta}(\sigma_t(\alpha)) \text{ with } \vec{\Sigma}_t(\vec{\zeta}(\alpha)) = \vec{\zeta}(\sigma_t(\alpha))$$

Numerical experiments: FB dynamic phantom

The phantom μ is an image (linear combination of pixel indicators).
$\mu_{\vec{\Gamma}_t}$ is dynamically deformed

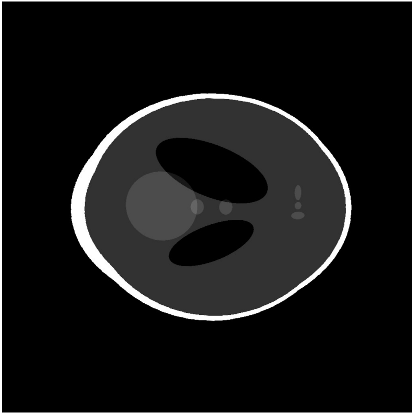

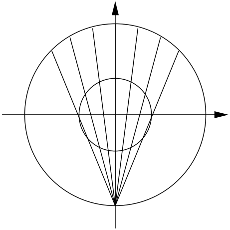

Figure: Dynamic Phantom FB $\phi = 0$

Numerical experiments: FB dynamic phantom

The phantom μ is an image (linear combination of pixel indicators).
$\mu_{\vec{\Gamma}_t}$ is dynamically deformed

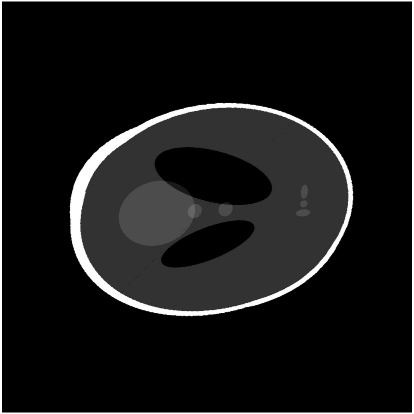

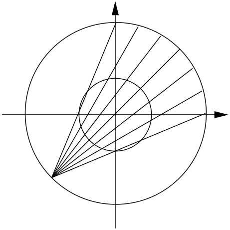

Figure: Dynamic Phantom FB $\phi = \frac{\pi}{4}$

Numerical experiments: FB dynamic phantom

The phantom μ is an image (linear combination of pixel indicators).
$\mu_{\vec{\Gamma}_t}$ is dynamically deformed

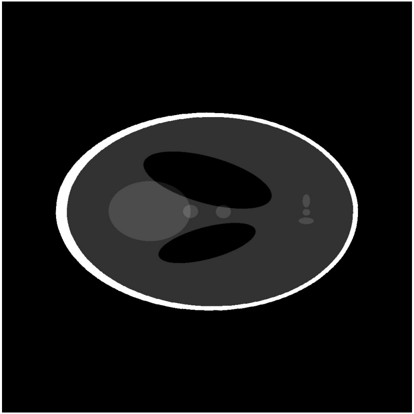

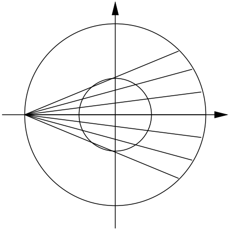

Figure: Dynamic Phantom FB $\phi = \frac{\pi}{2}$

Numerical experiments: FB dynamic phantom

The phantom μ is an image (linear combination of pixel indicators).
$\mu_{\vec{\Gamma}_t}$ is dynamically deformed

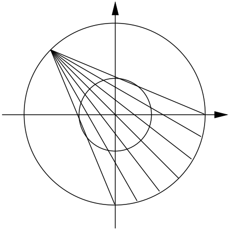

Figure: Dynamic Phantom FB $\phi = \frac{3\pi}{4}$

Numerical experiments: FB dynamic phantom

The phantom μ is an image (linear combination of pixel indicators).
$\mu_{\vec{\Gamma}_t}$ is dynamically deformed

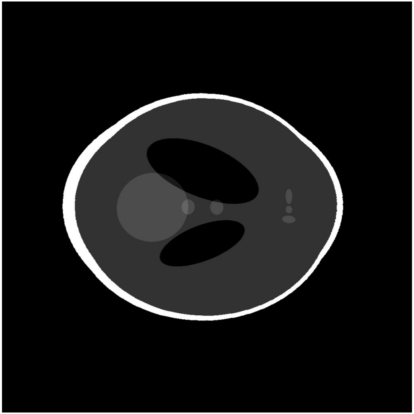

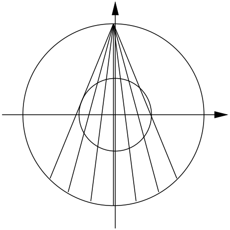

Figure: Dynamic Phantom FB $\phi = \pi$

Numerical experiments: FB dynamic phantom

The phantom μ is an image (linear combination of pixel indicators).
$\mu_{\vec{\Gamma}_t}$ is dynamically deformed

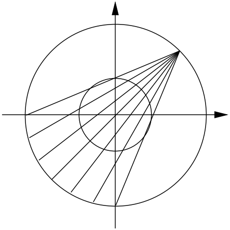

Figure: Dynamic Phantom FB $\phi = \frac{5\pi}{4}$

Numerical experiments: FB dynamic phantom

The phantom μ is an image (linear combination of pixel indicators).

$\mu_{\vec{\Gamma}_t}$ is dynamically deformed

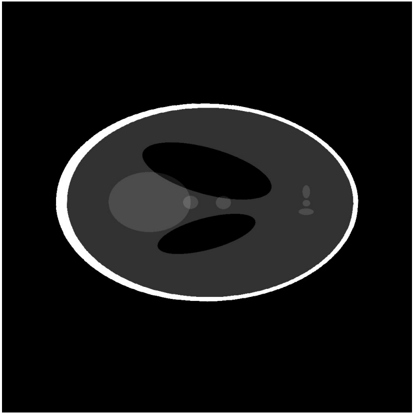

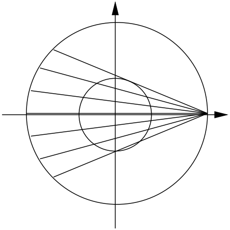

Figure: Dynamic Phantom FB $\phi = \frac{3\pi}{2}$

Numerical experiments: FB dynamic phantom

The phantom μ is an image (linear combination of pixel indicators).
$\mu_{\vec{\Gamma}_t}$ is dynamically deformed

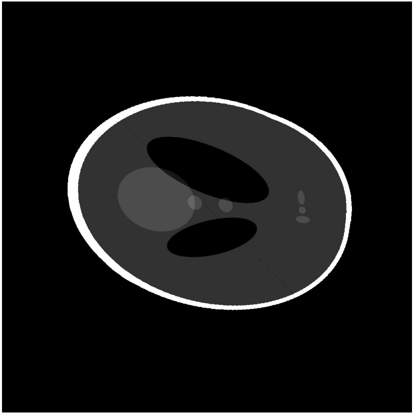

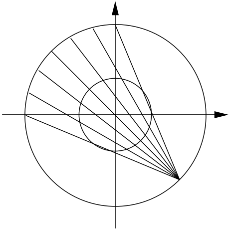

Figure: Dynamic Phantom FB $\phi = \frac{7\pi}{4}$

Numerical experiments: FB dynamic phantom

The phantom μ is an image (linear combination of pixel indicators).
$\mu_{\vec{\Gamma}_t}$ is dynamically deformed

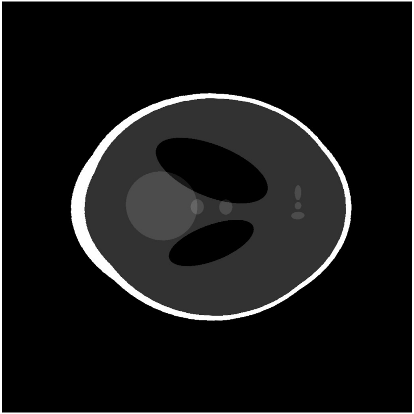

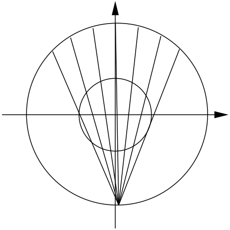

Figure: Dynamic Phantom FB $\phi = 2\pi - \Delta\phi$

SL: DBP reconstructions from full FB scann

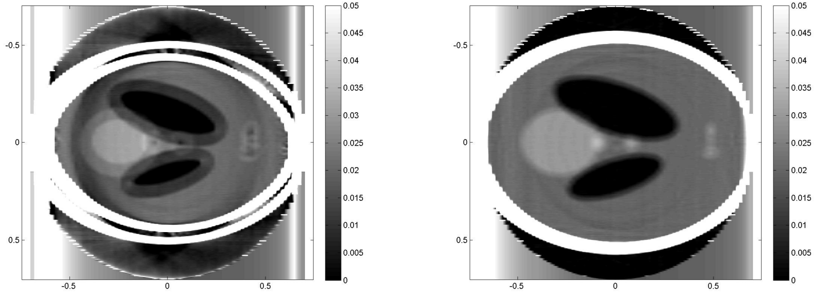

Figure: Left: NO compensation ; Right: Compensation (rebinning)

1024 angular projections, 1024 translations, $R = 3$

DBP reconstructions from FB truncated projections

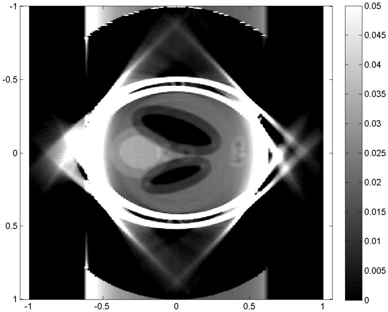

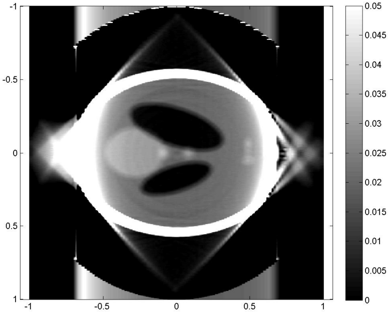

Figure: Left: NO compensation ; Right: Compensation (rebinning)

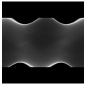

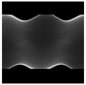

Summary

- Deformation preserving the acquisition geometry takes care for the Radon Transform.
- Mass preservation takes care for variable changes
- Mass and acquisition line geometry preservation yields a rebinning formula
- ROI reconstruction in the virtual trajectory
- Future work: more numerical experiments + 3D

Thank you! Questions ?

Thank you for your attention!
Questions ?

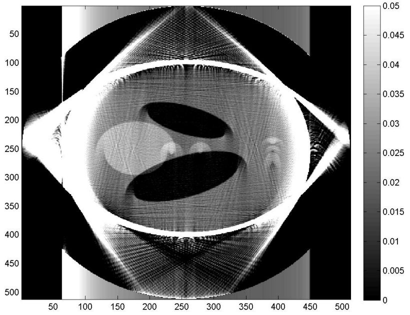

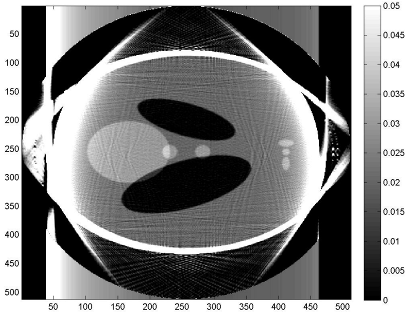

Density, mass and geometry conservation

Because organs are essentially incompressible, we can write the density conservation $\mu_{\vec{\Gamma}_t}(\vec{x}) = \mu\left(\vec{\Gamma}_t(\vec{x})\right)$. For mass and geometry conservative deformations this yields $|\gamma'_{t,\vec{\zeta}}(l)||J_{\vec{\Sigma}_t}(\vec{\zeta})|\frac{\gamma^{d-1}_{t,\vec{\zeta}}(l)}{l^{d-1}} = 1$

Proposition

A time dependent deformation preserving the divergent geometry and the mass preserves the density iff

$$\gamma_{t,\vec{\zeta}}(l) = c_t(\alpha)l \text{ and } \psi'_t(\alpha) = \frac{1}{c_t^2(\alpha)}$$

with $c_t(\alpha) > 0$ *some* 2π*-periodic smooth function such that* $\int_0^{2\pi} \frac{d\alpha}{c_t^2(\alpha)} = 2\pi$.

Line integral model

For line integral model, "mass preserved on the line" if

$$\mu_{\vec{\Gamma}_t}\left(\vec{v}(t)+l\vec{\zeta}\right)=\mu\left(\vec{\Gamma}_t\left(\vec{v}(t)\right)+\gamma_{t,\vec{\zeta}}(l)\vec{\Sigma}_t(\vec{\zeta})\right)|\gamma'_{t,\vec{\zeta}}(l)|$$

then

$$\begin{aligned}\int_{\mathbb{R}^+}\mu_{\vec{\Gamma}_t}\left(\vec{v}(t)+l\vec{\zeta}\right)dl &= \int_{\mathbb{R}^+}\mu\left(\vec{\Gamma}_t\left(\vec{v}(t)\right)+\gamma_{t,\vec{\zeta}}(l)\vec{\Sigma}_t(\vec{\zeta})\right)|\gamma'_{t,\vec{\zeta}}(l)|dl\\ &= \int_{\mathbb{R}^+}\mu\left(\vec{\Gamma}_t\left(\vec{v}(t)\right)+l\vec{\Sigma}_t(\vec{\zeta})\right)dl\end{aligned}$$

thus

$$\mathcal{D}\mu_{\vec{\Gamma}_t}\left(\vec{v}(t),\vec{\zeta}\right)=\mathcal{D}\mu\left(\vec{\Gamma}_t\left(\vec{v}(t)\right),\vec{\Sigma}_t(\vec{\zeta})\right)$$

Static versus dynamic compensated

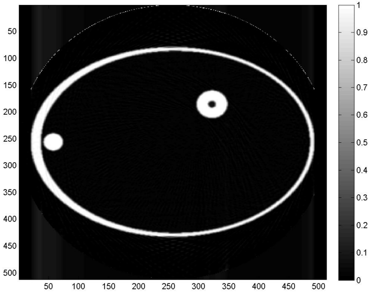

Figure: Left: Static (Full data) DBP ; Right: Dynamic (Truncated data)Corr DBP

Bibliography

Clackdoyle, R., & Defrise, M. 2010.
Tomographic Reconstruction in the 21st century.
IEEE Signal Processing Magazine, **27**(4), 60–80.

Crawford, C.R., King, K.F., Ritchie, C.J., & Godwin, J.D. 1996.
Respiratory compensation in projection imaging using a magnification and displacement model.
IEEE Transactions on Medical Imaging, **15**, 327 –332.

Flohr, T., & Ohnesorge, B. 2001.
Heart rate Adaptative Optimization of Spatial and Temporal Resolution for Electrocardiogram-Gated Multislice Spiral CT of the Heart.
Journal of Computer Assisted Tomography, **25(6)**, 907–923.

Gilland, D. R., Mair, B. A., Bowsher, J. E., & Jaszczak, R. J. 2002.
Simultaneous reconstruction and motion estimation for gated cardiac ECT.
IEEE Transactions on Nuclear Sciences, **49**(October), 2344–2349.

Grangeat, P., Koenig, A., Rodet, T., & Bonnet, S. 2002.
Theoretical framework for a dynamic cone-beam reconstruction algorithm based on a dynamic particle model.
Phys. Med. Biol., **47**(15), 2611–2625.

Kachelriess, M., & Kalender, W. A. 1998.
Electrocardiogram-correlated image reconstruction from subsecond spiral computed tomography scans of the heart.
Medical Physics, **25(12)**(December), 2417–2431.

Kachelriess, M., Ulzeimer, S., & Kalender, W. A. 2000.
ECG-correlated reconstruction from subsecond multi-slice spiral CT scans of the heart.
Medical Physics, **27(5)**(August), 1881–1902.

Krimski, S., & et al. 2005.
Respiratory correlated cone-beam computed tomography on an isocentric C-arm.
Phys. Med. Biol., **50**(22), 5263–80.